September 1997

Two-arm manipulation tasks with friction assisted grasping

Jaydev P. Desai
University of Pennsylvania

Milos Zefran
University of Pennsylvania

R. Vijay Kumar
University of Pennsylvania, kumar@grasp.upenn.edu

Postprint version. Published in *Proceedings of the Conference on Intelligent Robot Systems (IROS'97)*, September 1997.

Two-arm manipulation tasks with friction assisted grasping

Abstract

The main objective of this paper is to study human dual arm manipulation tasks and to develop a computational model that predicts the trajectories and the force distribution for the coordination of two arms moving an object between two given positions and orientations in a horizontal plane. Our ultimate goal is to understand the dynamics of human dual arm coordination in order to develop better robot control algorithms.

The first important observation is that the trajectories show a significant degree of repeatability across trials and across subjects. Secondly, we observe that the trajectories in the sagittal and frontal plane are characterized by asymmetric features that are hard to model using such integral cost functions. We propose a computational model based on the hypothesis proposed by Uno *et al.* [1] that suggests that human movements minimize the integral of the norm of the rate of change of actuator torques. We compare the experimental trajectories and force distributions with this computational model. We show that the internal forces play an important role in trajectory generation. While these are repeatable across trials, they vary significantly from subject to subject.

Comments

Postprint version. Published in *Proceedings of the Conference on Intelligent Robot Systems (IROS'97)*, September 1997.

Two-arm manipulation tasks with friction assisted grasping *

Jaydev P. Desai, Miloš Žefran and Vijay Kumar
General Robotics and Active Sensory Perception (GRASP) Laboratory, University of Pennsylvania
3401 Walnut Street, Room 301C, Philadelphia, PA 19104-6228

Abstract

The main objective of this paper is to study human dual arm manipulation tasks and to develop a computational model that predicts the trajectories and the force distribution for the coordination of two arms moving an object between two given positions and orientations in a horizontal plane. Our ultimate goal is to understand the dynamics of human dual arm coordination in order to develop better robot control algorithms.

The first important observation is that the trajectories show a significant degree of repeatability across trials and across subjects. Secondly, we observe that the trajectories in the sagittal and frontal plane are characterized by asymmetric features that are hard to model using such integral cost functions. We propose a computational model based on the hypothesis proposed by Uno *et al.* [1] that suggests that human movements minimize the integral of the norm of the rate of change of actuator torques. We compare the experimental trajectories and force distributions with this computational model. We show that the internal forces play an important role in trajectory generation. While these are repeatable across trials, they vary significantly from subject to subject.

1 Introduction

This paper is primarily concerned with the coordination and cooperation between two physically coupled arms in a task which requires positioning and orienting an object in a horizontal plane using an open-palm, friction-assisted grasp. The two palms must "squeeze" the object to generate frictional forces that will equilibrate the weight. In addition, the palms must exert forces that will move the object from a given position to another specified position. Because there are many trajectories that can be followed and because the force distribution (squeeze force) is not unique, the problem of generating motions is indeterminate. The goal of this paper is to study human manipulation and investigate optimality criteria that may describe (model) formation of trajectories and the distribution of forces. If such an optimality criterion can be found, it may be used to develop an appropriate coordination strategy for cooperating robot arms.

The coordination of cooperating robot arms has been studied extensively in the robotics literature. In most previous work, it is assumed that the trajectory of the object is prespecified and the focus has been on on-line control schemes for load sharing between the two robots [2, 3, 4, 5]. In these studies, the actuator redundancy is resolved by locally minimizing a suitable cost function which usually involves some measure of the internal forces. In contrast to these methods which achieve point-wise optimality, it is possible to pursue globally optimal solutions. Much of the work on cooperating arms ignores the dynamics of the grasp. While Yun [6] and Erdmann [7] consider the control and planning of manipulation with open-palm grasps, neither paper addresses the planning of trajectories and forces.

Many previous studies have investigated mechanisms that might underlie the generation of single arm trajectories in humans [1, 8, 9, 10, 11]. Flash and Hogan [9] study single arm reaching tasks and suggest that the central nervous system (CNS) uses *minimum-jerk* solutions. According to studies on coordinated manipulation with two arms by humans [12], it appears that the minimum-jerk criterion may not adequately explain trajectory formation in such tasks. Garvin *et al.* present experimental results showing that the rotational and translational componenets of motion are independently planned in the workspace and that they are combined in a hierarchial fashion to produce the observed behavior. They further hypothesize that the CNS reduces the multiple degrees of freedom motion planning problem into several simpler independent problems. In our earlier work [13], we have discussed the optimization of trajectories and distribution of forces for two cooperating arms in artificial and biological systems. The observed trajectories for frontal and sagittal plane motions were roughly straight lines and the velocity profiles were bell-shaped with a good degree of repeatability.

Kawato [14], proposes an alternative cost function for trajectory generation. This function is the integral of the norm of the vector of derivatives of the actuator torques along the trajectory; hence the name

*We gratefully acknowledge the support of NSF grant CMS91-57156, and ARO grant DAAH04-96-1-0007 . The first author is also supported by a Fellowship (NSF grant SHR89-20230) from the Institute for Research in Cognitive Science at the University of Pennsylvania.

minimum torque-change criterion. The main difference from minimizing the jerk is that the dynamics of the system must be considered while calculating the optimal solution. In a previous paper [15], we study different integral cost functions for dual arm robot manipulation tasks. The solution of the resulting optimal control problem yields not only the optimal trajectory but also the optimal internal forces.

In this paper, we study the task of positioning and orienting an object with two arms at a visually specified goal position and orientation in the horizontal plane. The grasp consists of the two palms contacting the object on flat rough surfaces as shown in Fig. 1. Motion planning for this case is more complicated than for the single arm case since it involves three degrees of freedom (two translational and one rotational) and must take into account the constraints imposed by the physical coupling of the two arms (through the object). Motivated by the kinematic analysis of the experimental data [12] and by the findings from [13], we only consider minimum torque-change model. The trajectories and force distributions obtained by optimization are compared to experimental observations of human two-arm manipulation tasks.

2 Experimental system

The experimental system for measuring trajectories and force distribution consists of a target system and a passive planar manipulandum with a handle as shown in Fig. 1. The sides of the handle are parallel plates and simulate a box-like object. Metallic tabs can be added to the handle in order to vary its weight and inertia. Each plate is instrumented with a six-axis force/torque sensor allowing measurement of the forces and torques exerted by the subject during the manipulation task. The handle assembly is attached to the manipulandum with a low-friction, linear bearing. Thus, during the experiment, the weight of the object is supported by the two palms and not by the manipulandum.

The manipulandum consists of three links, connected by revolute joints. The first two links of the manipulandum form a serial kinematic chain capable of locating the distal end of the second link (which coincides with the center of the third link) at any position (x, y) in the horizontal plane (two degrees of freedom) within the manipulandum workspace. By revolving about its center point, the third link (the handlebar) provides a third, rotational degree of freedom (ϕ). Three optical encoders mounted at the joints are used to measure the corresponding angles of rotation at a sampling rate of 200 Hz. During the experiments, the subject sits in front of the manipulandum, and firmly grasps the two flat plates of the handle as shown in Fig. 1. A rectangular wooden frame supporting a transparent Plexiglas sheet is suspended from the ceiling by nylon cables, such that the Plexiglas sheet is horizontal at the level of the subject's chin (Fig. 1).

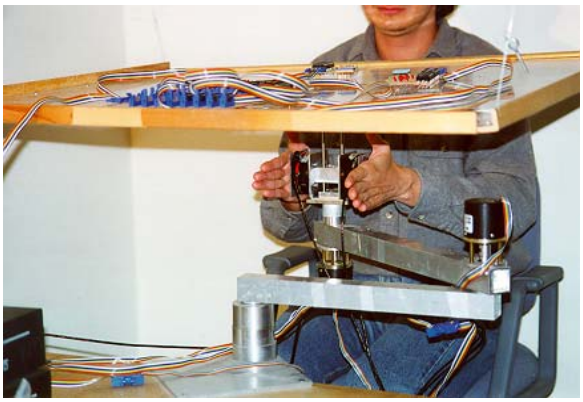

Figure 1: Experimental testbed

Four target sets are mounted on the Plexiglas at different locations, and each set consists of arrays of light emitting diodes (LEDs). The geometry and position of the diodes is as shown in Fig. 2.

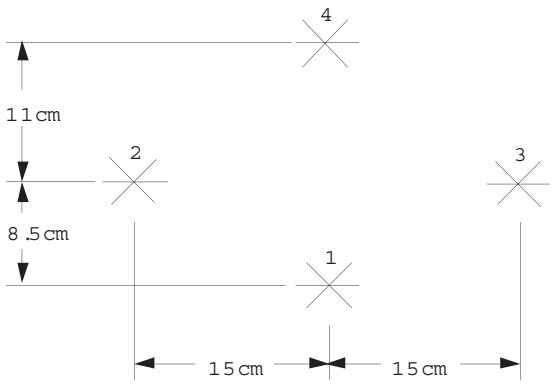

Figure 2: The system of targets

The room was darkened, and a random sequence of target configurations was presented. The duration during which any given target was lit was also randomly determined in the range 1.5 - 3.5 seconds. The subjects were instructed to position and orient the handlebar at the configuration specified by the lit array of LED's, while maintaining a firm grasp on the side plates with both hands and keeping the elbows in the horizontal plane passing through the shoulders. They were told to move naturally, i.e. at what was in their opinion a comfortable speed. High accuracy was not required from the subjects, as they were instructed not to be unduly concerned about small errors in final location. Furthermore, since the experiments were performed in the dark, no visual feedback of the arms and the handle was provided to the subjects. Some of the subjects commented that they were able to see the handle after they adapted to the darkness. Each subject was asked to perform five groups of fifty movements. Four healthy subjects participated in the experiments, ages ranging between 24 and 40. The

first fifty motions from each subject were discarded allowing the subject to adapt to the experimental task (though they were not informed that the first fifty motions would be discarded). The recorded encoder readings were analyzed off-line, and the corresponding joint angles of the manipulandum were derived after the data was processed with a third order Butterworth low pass filter using a cutoff frequency of 7.5 Hertz. The corresponding angular velocities were obtained by numerical differentiation using a five-point Lagrangian difference method [16]. The Cartesian trajectories and velocity profiles of both handles (and both hands) were then derived by employing the forward kinematics transformations for the manipulandum.

For each measured motion, only those components for which the prescribed amplitudes were non-zero were considered (e.g., the rotational components of motions for which zero rotation was prescribed were discarded). Therefore, only components having high signal/noise ratio were used. These components are referred to as the "significant components" of motion. Considering each significant component separately, the start and end times were taken as the point in time when the velocity of that component has reached 5% of its peak velocity. For a given motion, the minimum of the start times of its significant components was taken as the motion start time, and the maximum of their end times was taken as the motion's end time.

In order to compare motions of different durations, amplitudes and directions, the durations and amplitudes were normalized [8, 11]. For each motion, the normalized duration (τ) was:

$$\tau = (t - t_0)/(t_f - t_0)\ . \tag{1}$$

Similarly, for each motion component (e.g., x), the normalized amplitude ($\hat{x}$) was taken as

$$\hat{x} = (x(t) - x(t_0))\ /\ (x(t_f) - x(t_0))\ . \tag{2}$$

In order to normalize the velocity profiles, Eq. (2) was differentiated with respect to normalized time. Since

$$d\hat{x}/d\tau = (d\hat{x}/dt)\ \ (dt/d\tau) \tag{3}$$

and

$$dt/d\tau = t_f - t_0\ , \tag{4}$$

it follows that

$$d\hat{x}/d\tau = \dot{x}\ \ (t_f - t_0)\ /\ (x(t_f) - x(t_0))\ . \tag{5}$$

3 A computational model for motion generation

We model the two arms holding an object in the horizontal plane by two planar 3-link manipulators as shown in Fig. 3. Each arm has 3 degrees of freedom. If the arms rigidly hold the object, the system of the two arms and the object has mobility 3. The object can therefore be placed at an arbitrary position and orientation in the plane. The closed loop is modeled by equality constraints on the position variables and the friction-assisted grasp by inequality constraints on the contact forces. The dynamics of the two manipulators can be described by two sets of three ordinary differential equations:

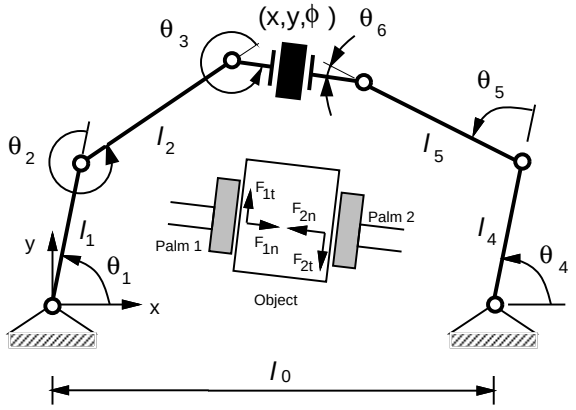

Figure 3: Two robots holding an object.

$$\begin{aligned} I_1(\theta_1)\ddot{\theta}_1 + C_1(\theta_1, \dot{\theta}_1) &= \tau_1 - \Gamma_1^T F_1 \\ I_2(\theta_2)\ddot{\theta}_2 + C_2(\theta_2, \dot{\theta}_2) &= \tau_2 - \Gamma_2^T F_2 \end{aligned} \tag{6}$$

where θ_i is the 3×1 vector of the joint coordinates of the ith ($i = 1, 2$) manipulator, $I_i(\theta)$ is the 3×3 inertia matrix, $C_i(\theta_i, \dot{\theta}_i)$ is the 3×1 vector of nonlinear terms (Coriolis and centrifugal forces), τ_i is the 3×1 vector of the joint torques, Γ_i is the 3×3 Jacobian matrix relating the velocity of the center of mass of the object to the joint velocities and F_i is the 3×1 generalized force vector, representing the force exerted by the manipulator on the object and the moment about the center of mass. The dynamics of the object is given by:

$$M\ddot{p} = F_1 + F_2 \tag{7}$$

where, M is the 3×3 inertia matrix of the object and $p = [x,\ y,\ \phi]^T$, is the 3×1 vector representing the position/orientation of the object with (x, y), being the coordinates of the position of the center of the object. As shown in Fig. 3, the components of the contact force acting on the object along the inward pointing normals are denoted by F_{1n} and F_{2n} while those tangential to the contact plane with F_{1t} and F_{2t}.

The two manipulators completely restrain the motion of the object. Therefore, the position of the center of mass of the object can be expressed as either a function of θ_1 or a function of θ_2 and the two functions must give the same value:

$$p_1(t) = p_2(t) \tag{8}$$

where the vector p_1 denotes the position and orientation of the object expressed as function of θ_1 and p_2 is the same vector expressed as function of θ_2.

The constraints on the normal component of the contact force are:

$$F_{1n} \geq 0, \qquad F_{2n} \geq 0. \tag{9}$$

The tangential forces are subject to constraints due to Coulomb's law of friction:

$$|F_{1t}| \leq \mu F_{1n}, \qquad |F_{2t}| \leq \mu F_{2n} \tag{10}$$

where μ is the coefficient of friction.

The system of the object and the two manipulators contains 6 actuators but the object only has 3 degrees of freedom. Consequently, the task is overconstrained. There are infinitely many possible force and motion trajectories that achieve the desired motion of the object from the initial configuration to the desired final configuration.

To find a unique solution, we adopt the optimal control strategy first proposed by Uno and Kawato [1, 14]. In a previous paper [13], we showed that this computational model adequately explains some features of two-arm motions with form-closed grasps. For the task proposed here, this optimality criterion reduces to the minimization of the rate of change of the actuator torques over the trajectory:

$$\min \quad \frac{1}{2} \int_{t_0}^{t_f} (\dot{\tau}_1^2 + \dot{\tau}_2^2)\, dt \tag{11}$$

subject to the constraints in Equations (6-10).

We define the input vector to be

$$u = \dot{\tau}. \tag{12}$$

In order to write the dynamic equations of motion in standard state space notation, we define a state vector

$$x = \begin{bmatrix} x_1 \\ x_2 \\ x_3 \end{bmatrix} = \begin{bmatrix} p \\ \dot{p} \\ \tau \end{bmatrix}, \tag{13}$$

where p is a 3×1 vector consisting of the Cartesian coordinates of the center (P) of the object (handle) and its orientation, and $\dot{p}$ is the corresponding Cartesian velocity vector. The system dynamics in (6,12) can be rewritten as 12 first order differential equations:

$$\begin{bmatrix} \dot{x}_1 \\ \dot{x}_2 \\ \dot{x}_3 \end{bmatrix} = \begin{bmatrix} x_2 \\ A(x_1, x_2) + B(x_1)x_3 \\ 0 \end{bmatrix} + \begin{bmatrix} 0 \\ 0 \\ I \end{bmatrix} u \tag{14}$$

where $A(x_1, x_2)$ is a 3×3 matrix consisting of position and velocity dependent inertial terms and $B(x_1)$ is a 3×6 Jacobian matrix. This standard approach is described in greater detail in [6, 17].

Boundary conditions must be specified to solve the optimal control problem defined by (11,14). For each movement, we know the start and end positions. Further, the motion starts and ends with zero velocity and acceleration. Thus we have a total of 9 boundary conditions at each point. Since we have a 12-dimensional state space, we can specify 3 additional boundary conditions at each end [15]. For example, it may be meaningful to specify the internal forces at the beginning and the end of the maneuver.

The theoretical development for solving optimal control problems with state constraints is detailed in [18].

4 Results

In this paper, we study motions in which the initial and goal orientations are the same. In other words, it is possible for the subject to go from the initial to the final position via a pure translation, although the experimental apparatus allows the subject to perform rotations as well. The trajectories and force histories for four subjects are presented and analyzed.

Repeatability

During the experiments, the time taken to complete the motion varied from 0.8 seconds to 1.2 seconds, and there is considerable variation across subjects. Further, the subjects made a systematic error when reaching the targets. This was expected given that no visual feedback of the arms with the handle was provided and because of the parallax in the perception of the target. However, the duration of the motion and the accuracy in reaching the target are of secondary importance to this study since we are primarily interested in the kinematic and dynamic features of the measured trajectories.

We tested the repeatability of the trajectories by comparing the motions performed by the same subject and by different subjects on different trials. Numerical calculations of repeatability measures for different trajectories (within subject and across subjects) are presented in [12]. The velocity histories were found to be repeatable across trials for the same subject and across subjects. The results presented later in this paper will also demonstrate this point. Note that in all the experiments studied here, the angular variations (ϕ) and the torques recorded by the force/torque sensors are close to zero and will not shown in the plots.

Frontal and sagittal plane motions

The trajectories for a representative subject for the $3 \rightarrow 2$ and the $4 \rightarrow 1$ motions (the numbers refer to the target numbers in Fig. 2) are shown in Figures 4 and 5. The spread in the sagittal plane trajectories ($4 \rightarrow 1$) can be seen to be less than 0.01 meters while the spread in the frontal plane trajectories ($3 \rightarrow 2$) is less than 0.05 meters. At first sight, it appears that the trajectories are straight lines, but it is clear from Figures 4(b) and 5(b), that the average trajectory is curved. This is also the case for motions in the opposite direction, $1 \rightarrow 4$ and $2 \rightarrow 3$, as shown in Fig. 6. In fact, if we compare the trajectories for $1 \rightarrow 4$ and $4 \rightarrow 1$, and similarly for $2 \rightarrow 3$ and $3 \rightarrow 2$, we find

that the curvatures have opposite signs. The average curvature for these trajectories is shown in Table 1 for subjects S1-S4. While the signs of the curvature for the trajectories was observed to be the same across subjects, there was a significant variability in the actual values. However, the variability for one subject across trials was found to be very low. For example, for subject S2, the standard deviation in the curvature for the $4 \rightarrow 1$ motion and the $3 \rightarrow 2$ motion was observed to be 0.0035 meters and 0.0098 meters.

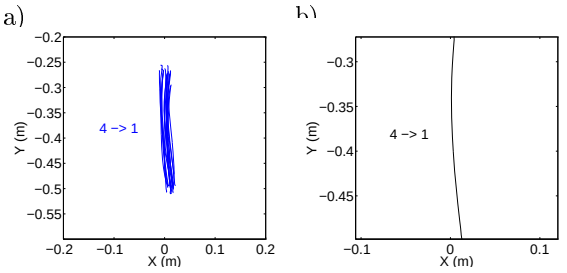

Figure 4: a) Observed trajectories and b) Average trajectory for the $4 \rightarrow 1$ motion.

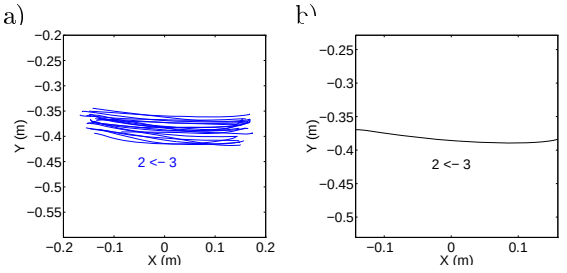

Figure 5: a) Observed trajectories and b) Average trajectory for the $3 \rightarrow 2$ motion.

Table 1: Radius of curvature for motions in the frontal and sagittal planes.

Motion	S1	S2	S3	S4
$2 \rightarrow 3$	$-0.53m$	$-0.48m$	$-0.45m$	$-0.46m$
$3 \rightarrow 2$	$+0.53m$	$+0.57m$	$+0.61m$	$+0.59m$
$4 \rightarrow 1$	$+0.49m$	$+0.50m$	$+0.50m$	$+0.49m$
$1 \rightarrow 4$	$-0.52m$	$-0.51m$	$-0.52m$	$-0.51m$

The bias in curvature was not statistically significant in oblique translatory motions. The average trajectories for the $2 \rightarrow 4$ and $1 \rightarrow 3$ motions are shown in Fig. 7. From the individual plots (not all are shown in this paper), we found the $1 \rightarrow 3$ trajectories to be less curved than all other trajectories.

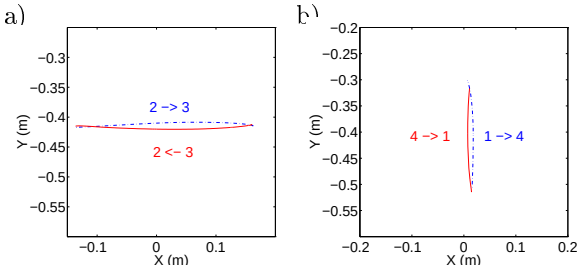

Figure 6: Trajectories for: a) the $2 \rightarrow 3$ and $3 \rightarrow 2$ motions; and b) the $1 \rightarrow 4$ and $4 \rightarrow 1$ motions.

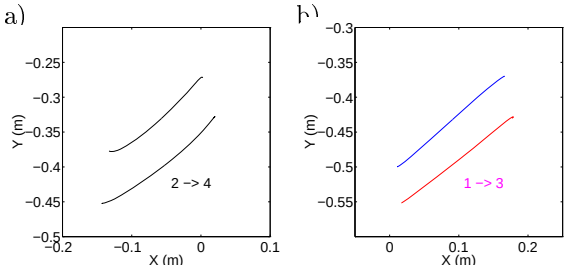

Figure 7: Trajectories for: a) the $2 \rightarrow 4$ motion; and b) the $1 \rightarrow 3$ motion.

Force history

As the total (resultant) force acting on the object is uniquely determined by the trajectories, we will be mainly interested in the internal forces. There are three components to the internal force vector: a moment perpendicular to the plane and two force components. We will denote the internal force in the direction normal to the two palms by F_n, where

$$F_n = F_{1n} - F_{2n}.$$

We will call this component the *interaction force*, using the terminology of [3]. The tangential component and the moment normal to the plane are observed to be negligible in this study and are not discussed further.

The internal forces varied significantly across subjects. While the instructions for the task (moving from one target to another) specify the initial and final positions and velocities, there is no mechanism for specifying the initial and final internal forces. Each subject used a different initial and final internal (grip) force and therefore, there is considerable variability in the magnitudes across subjects. For this reason we did not average the internal force data across subjects.

The internal force history for the motion ($2 \rightarrow 3$) is shown in Fig. 8a for two representative subjects. The solid line denotes the subject, S3, and the dashed line denotes the subject, S4. The internal force increased as the velocity increased to a peak and then decreased toward the end of the motion. While the magnitude of the internal force varied across subjects, this general trend was observed in all subjects.

The normal component of the forces exerted on the object are shown in Fig. 8b. In the $2 \rightarrow 3$ motion,

there was an initial dominance by the left arm followed by a right arm dominance in the second half of motion. In other words, the palm that pushed the object in the direction of acceleration or deceleration dominated. This is consistent with the observations of Reinkensmeyer *et al.* [19] in their study of bimanual, single-degree-of-freedom, wrist movements. However, the forces exerted by the left arm were larger than the right arm. This can be easily explained if we look at the data of [13, 12, 20] that shows that the velocity profiles (not shown here) are always asymmetric. The time taken to go from zero velocity to the maximum velocity is always less than the time taken to decelerate from the peak velocity to rest. In other words, the magnitude of the peak acceleration (to the right), is always lower than the magnitude of the peak deceleration (to the left). Since, in the $2 \rightarrow 3$ motion, the hand that dominates initially (the pushing hand) is the left hand, we expect to find the left arm force to be larger than the right arm force.

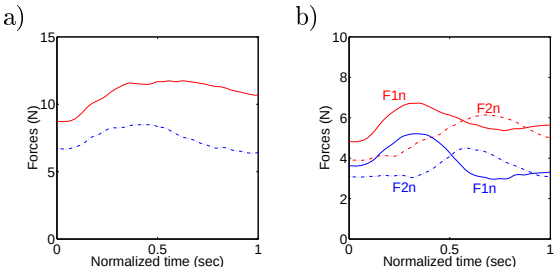

Figure 8: a) Internal forces and (b) left and right palm forces for the $2 \rightarrow 3$ motion for subjects S3 (solid) and S4 (dashed).

The internal force for the sagittal plane motions are shown in Fig. 9. During the $4 \rightarrow 1$ motion, once again there was an increase in the internal force F_n, as the object was moved from the initial to final position. However, the increase was more significant and occured through a larger part of the motion than observed for frontal plane motions (Fig. 8). This initial increase was also seen when the object was moved from $1 \rightarrow 4$ as shown in Fig. 10. However, in this case the increase was followed by a significant decrease in the internal force.

Thus, there are two general trends observed in Figs. 8a and 10. As mentioned earlier, the internal force appeared to increase as the velocity of the object increased. In addition, the internal force increased as the object was moved closer to the subject and decreased as the object was moved away.

4.1 General translatory motions

The trajectories in the frontal plane and those in the sagittal plane showed a tendency to curve, and this tendency was consistent across trials with the same subject and across subjects. In general translatory motions, the curvature in the observed trajectories was not consistent across subjects. However, the exception is the trajectory for the motion $1 \rightarrow 3$ which was found to be straight for all subjects. The average trajectory and the average velocity profiles for this motion are shown in Fig. 11. Because the trajectory was very close to a straight line, the velocities in the x and y direction were the same except for a scaling factor. Neither of these two observations could be made for any other oblique motion. Further the $1 \rightarrow 3$ trajectory and the force distribution appeared to be more repeatable than for other oblique motions. The average internal force profile and the palm force profiles for the $1 \rightarrow 3$ motion are shown for two different subjects in Fig. 12. Once again, the internal forces and the left and right arm forces show the same trends observed earlier. The internal force increased as the velocity increased and then decreased toward the end of the motion. Also, the dominance of the left arm force in the beginning and the right arm toward the end was clearly seen for both the subjects in Fig. 12b.

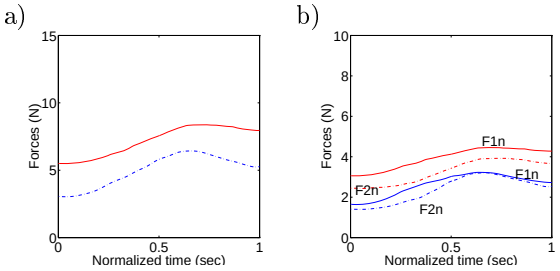

Figure 9: a) Internal forces and (b) left and right palm forces for the $4 \rightarrow 1$ motion for subjects S3 (solid) and S4 (dashed).

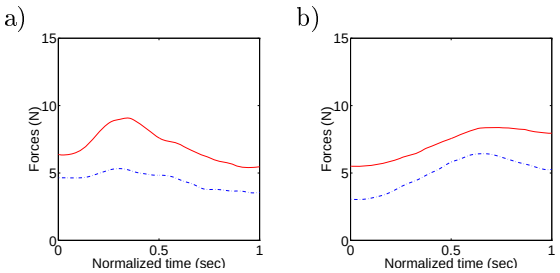

Figure 10: Internal forces for (a) the $1 \rightarrow 4$ motion and (b) the $4 \rightarrow 1$ motion for S3 (solid) and S4 (dashed).

4.2 Computational results and experimental observations

In this subsection, we compare the experimental observations with the predictions from the computational model for the $1 \rightarrow 3$ oblique motion. Instead of using the averaged results, we randomly chose an experimental trial[1] for comparison. The boundary con-

[1] Since we need boundary conditions to generate the solution to (6-11), we use experimentally observed end conditions rather than averaged boundary conditions.

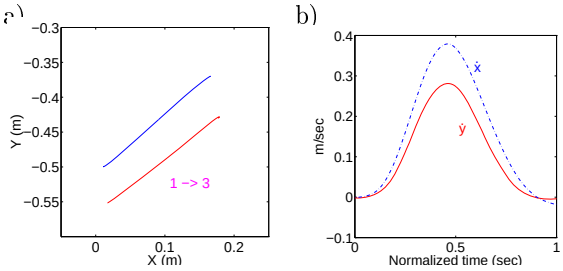

Figure 11: a) Average trajectory; and b) average velocity profiles for the $1 \rightarrow 3$ motion.

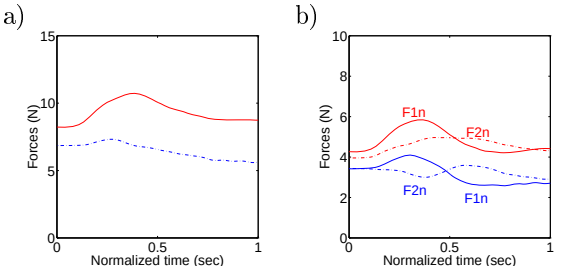

Figure 12: a) Internal forces and (b) left and right palm forces for the $1 \rightarrow 3$ motion for S3 (solid) and S4 (dashed).

ditions (initial and final position, velocity, acceleration and interaction force) for the computational model are calculated from the experimental data.

The predicted and observed trajectory is shown in Fig. 13a. and the velocities are shown in Fig. 14. The discrepancy between the theoretical predictions and the experimental data is small compared to the variance of the data (not shown in the plots). However, this is not true of the interaction force shown in Fig. 13b. The predicted variation of the interaction force is very small. However, the experimental data shows that the interaction force first increases and then tails off. In particular, the computational model does not capture the increase in interaction force with an increase in object velocity.

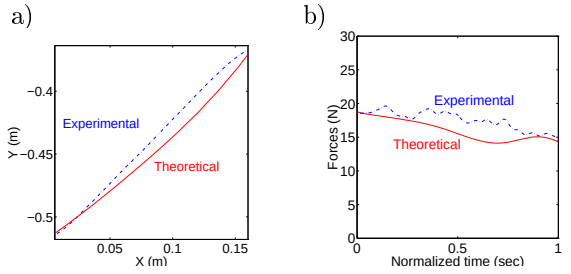

Figure 13: Theoretical and experimental a) Trajectory and b) Interaction force for motion $1 \rightarrow 3$

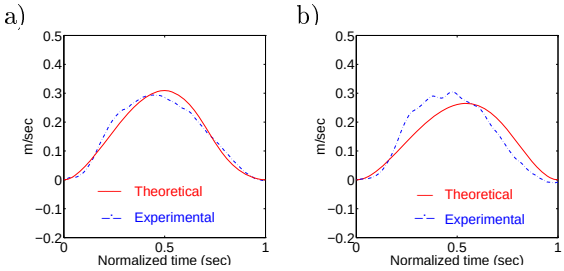

Figure 14: Theoretical and experimental velocities: a) $\dot{x}$ and b) $\dot{y}$ for motion $1 \rightarrow 3$

4.3 Effect of increasing the weight of the grasped object

If the object is made heavier, one would expect the internal force to increase so that the ratio of the tangential to the normal force at each palm is less than the coefficient of friction. Fig. 15 shows the effect of increasing the mass of the object from 0.85 to 1.95 Kgs for two representative motions for one subject averaged across all trials. Increasing the payload resulted in an increase in the internal force but there was no significance change in the trajectory.

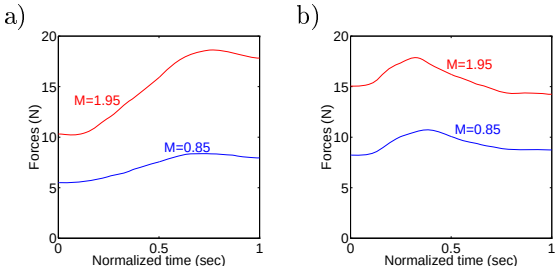

Figure 15: Internal force plots for motion a) $4 \rightarrow 1$ and b) $1 \rightarrow 4$ for S3 (solid) and S4 (dashed).

5 Discussion

There are many trajectory generation and motion planning schemes that have been proposed for cooperating robot arms in the literature. However, there is no clear rationale for selecting one method over another. In this paper, we study human manipulation tasks with the goal of improving our understanding of human coordination and control. The motivation is to see if such an understanding can help in the development of a superior coordination algorithm for robot arms.

The first thing that is worth noting is that human trajectories and force distributions are surprisingly repeatable. This suggests that there is a definite strategy used by humans in manipulation tasks. The near-straightness of the trajectories and the smoothness of the velocity profiles suggest optimality by some measure. The increase in internal forces with an increased

external load (weight) suggests that the optimality criterion must incorporate the force distribution.

However, there are several observations that are difficult to explain with a simple optimality criterion. First, trajectories in the sagittal and frontal plane show a curvature that is consistent across subjects. This is particularly significant for manipulation in the sagittal plane. If the two arms are identical, there is no physical explanation for the asymmetry induced by this curvature. Clearly, the two arms are not identical. However there is no simple cost function that can model this asymmetry. Another significant observation that is difficult to explain using physical principles is the increase in internal force with an increase in velocity. One would expect internal forces to be larger for increased accelerations. However, this is not the case.

It is tempting to compare this work to the work on human grasping [19, 21, 22, 23]. It is worth noting that the internal forces in the experiments of [19, 21, 22, 23] are very high compared to the resultant force required to accelerate it. While the ratio of the grip force (equal to half the internal force in this paper) to the load force (equal to half the resultant force in this paper) in these papers varies from 3 to 7, this ratio in the bimanual task reported here is only around 1. For example, the peak internal force (F_n) for the $2 \rightarrow 3$ motion for subjects S3 and S4 was observed to be between 8N and 11N. The peak resultant force (F_R) was around 10N of which the weight of the grasped object accounted for 8.33N. It is also worth noting that weight accounts for a much larger fraction of the resultant force in our experiments.

Another difference between the experimental paradigm of this work and that used in previous studies has to do with the coupling between the grasping and the manipulation functions. In [21, 22, 23], the control of the grasp forces can be completely decoupled from the manipultion task because the joints and muscle groups used in manipulation are completely decoupled from those used in grasping. This is not true in our work and in [19], where the same effectors (palms) are responsible for holding the object and manipulating it.

We presented a computational model derived from the minimum-torque-change model for single-arm reaching tasks. The model predictions and the experimental findings were roughly consistent as far the trajectories and the velocities are concerned. However, the interaction forces were consistently different. Nevertheless if the asymmetry in the human neuromuscular system can be reflected in this model, it may serve as a model for predicting trajectories and force distribution in manipulation tasks. It can also be used for generating trajectories for synthetic human models in computer graphics and for motion planning in robotic systems. Finally, it is superior to previous trajectory planning models in that it explicitly incorporates the distribution of forces between the two arms and frictional constraints in friction-assisted grasps.

In this paper, we have provided a detailed analysis of planar manipulation tasks involving friction assisted grasps. The long term goal of this study is to see (a) if human trajectory formation and the distribution of forces between the arms can be explained by some optimality criterion; and (b) if such criteria can be used in the control and coordination of robotic arms. This study may also help improve our understanding of how humans use their arms in bimanual tasks. This is potentially useful for the design of haptic interfaces (and human-machine interfaces in general) in which two arms are required.

References

[1] Y. Uno, M. Kawato, and R. Suzuki, "Formation and control of optimal trajectory in human multijoint arm movement," *Biological Cybernetics*, vol. 61, pp. 89–101, 1989.

[2] Y. Zheng and J. Luh, "Optimal load distribution for two industrial robots handling a single object," in *IEEE International Conference on Robotics and Automation*, (Philadelphia, PA), Apr. 1988.

[3] X. Yun and V. Kumar, "An approach to simultaneous control of trajectory and interaction forces in dual-arm configurations," *IEEE Transactions of Robotics and Automation*, vol. 7, no. 5, 1991.

[4] D. Williams and O. Khatib, "The virtual linkage: a model for internal forces in multi-grasp manipulation," in *Proc. of 1993 IEEE Int. Conf. on Robotics and Automation*, (Atlanta, GA), 1993.

[5] K. Kreutz and A. Lokshin, "Load balance and closed chain multiple arm control," in *Proc. 1988 Amer. Control Conf.*, (Atlanta, GA), 1988.

[6] X. Yun, "Object handling using two arms without grasping," *The International Journal of Robotics Research*, vol. 12, pp. 99–106, feb 1993.

[7] M. Erdmann, "An exploration of nonprehensile two-palm manipulation: Planning and execution," in *Seventh International Symposium on Robotics Research*, oct 1995.

[8] P. Morasso, "Spatial control of arm movements," *Experimental Brain Research*, vol. 42, pp. 223–227, 1981.

[9] T. Flash and N. Hogan, "The coordination of arm movements: An experimentally confirmed mathematical model," *The Journal of Neuroscience*, vol. 5, no. 7, pp. 1688–1703, 1985.

[10] J. F. Soechting and F. Lacquaniti, "Invariant characteristics of a pointing movement in man," *The Journal of Neuroscience*, vol. 1, no. 7, pp. 710–720, 1981.

[11] C. G. Atkeson and J. M. Hollerbach, "Kinematic features of unrestrained vertical arm movements," *The Journal of Neuroscience*, vol. 5, no. 9, pp. 2318–2330, 1985.

[12] G. J. Garvin, M. Zefran, E. A. Henis, and V. Kumar, "Two-arm trajectory planning in a manipulation task," *Biological Cybernetics*, vol. 76, pp. 53–62, 1997.

[13] M. Žefran, V. Kumar, E. Henis, and J. Desai, "Two-arm manipulation: What can we learn by studying humans?," in *International Conference on Intelligent Robots and Systems*, (Pittsburg, USA), 1995.

[14] M. Kawato, "A bi-directional theory approach to prerational intelligence," in *Proceedings of ZiF Conference on Prerational Intelligence*, (Bielefeld, Germany), 1994.

[15] M. Žefran, V. Kumar, and X. Yun, "Optimal trajectories and force distribution for cooperating arms," in *Proceedings of the 1994 IEEE International Conference on Robotics and Automation*, (San Diego), 1994.

[16] F. B. Hildebrand, *Advanced Calculus for Applications*. Englewood Cliffs, NJ: Prentice-Hall, Inc., second ed., 1976.

[17] E. Paljug, X. Yun, and V. Kumar, "Control of rolling contacts in multi-arm manipulation," *IEEE Transactions on Robotics and Automation*, vol. 10, no. 4, 1994.

[18] J. P. Desai and V. Kumar, "Nonholonomic motion planning for multiple mobile manipulators," in *International Conference on Robotics and Automation*, (Albuquerque, NM), April 1997.

[19] D. J. Reinkensmeyer, P. S. Lum, and S. L. Lehman, "Human control of a simple two-hand grasp," *Biological Cybernetics*, vol. 67, pp. 553–564, 1992.

[20] J. P. Desai, M. Žefran, and V. Kumar, "Two-arm manipulation tasks with friction assisted grasping," in *International Conference on Intelligent Robots and Systems*, (Grenoble, France), Sept 1997.

[21] R. S. Johansson and G. Westling, "Roles of glabrous skin receptors and sensorimotor memory in automatic control of precision grip when lifting rougher or more slippery objects," *Experimental Brain Research*, no. 56, pp. 550–564, 1984.

[22] R. S. Johansson, R. Riso, C. Hager, and L. Backstrom, "Somatosensory control of precision grip during unpredictable pulling loads," *Experimental Brain Research*, no. 89, pp. 181–191, 1992.

[23] J. R. Flanagan, J. Tresilian, and A. M. Wing, "Coupling of grip force and load force during arm movements with grasped objects," *Neuroscience letters*, no. 152, pp. 53–56, 1993.